

Laser ultrasonic evaluation of human dental enamel during remineralisation treatment

Hsiao-Chuan Wang^{1*}, Simon Fleming¹, Yung-Chun Lee², Michael Swain³, Susan Law¹,
Jing Xue³

¹ Institute of Photonics and Optical Science, School of Physics, University of Sydney, NSW 2006, Australia

² Department of Mechanical Engineering, National Cheng Kung University, Tainan City, Taiwan

³ Faculty of Dentistry, University of Sydney, NSW 2006, Australia

hsiao-chuan.wang@sydney.edu.au

Abstract: In this work a non-destructive laser ultrasonic technique is used to quantitatively evaluate the progressive change in the elastic response of human dental enamel during a remineralisation treatment. The condition of the enamel was measured during two weeks treatment using laser generated and detected surface acoustic waves in sound and demineralised enamel. Analysis of the acoustic velocity dispersion confirms the efficacy, as well as illuminating the progress, of the treatment.

©2011 Optical Society of America

OCIS codes: 120.3890 (Medical optics instrumentation); 120.4290 (Nondestructive testing); 280.3375 (Laser induced ultrasonics); 240.6690 (Surface waves); 120.0280 (Remote sensing and sensors); 170.1850 (Dentistry).

References

1. B. Krasse, "Biological factors as indicators of future caries", *International Dental Journal*, vol.38, no.4, pp.219-225, December 1988
2. A.I. Ismail, "Visual and visuo-tactile detection of dental caries", *Journal of Dental Research*, vol.83, pp.C56-C66, 2004
3. F. Feagin, T. Koulourides, W. Pigman, "The characterization of enamel surface demineralization, remineralization, and associated hardness changes in human and bovine material", *Archives of Oral Biology*, vol.14, no.12, pp.1407-1417, December 1969
4. S. Habelitz, S.J. Marshall, G.W. Marshall Jr, M. Balooch, "Mechanical properties of human dental enamel on the nanometre scale", *Archives of Oral Biology*, vol.46, no.2, pp.173-183, 2001
5. J.L. Cuy, A.B. Mann, K.J. Livi, M.F. Teaford, T.P. Weihs, "Nanoindentation mapping of the mechanical properties of human molar tooth enamel", *Archives of Oral Biology*, vol.47, no.4, pp.281-291, April 2002
6. F. Lippert, D.M. Parker, K.D. Jandt, "In vitro demineralization/remineralization cycles at human tooth enamel surfaces investigated by AFM and nanoindentation", *Journal of Colloid and Interface Science*, vol.280, no.2, pp.442-448, December 2004
7. E. Soczkiewicz, "The Penetration Depth of the Rayleigh Surface Waves", *Nondestructive Testing and Evaluation*, vol.13, pp.113-119, 1997
8. J.D. Achenbach, *Wave Propagation in Elastic Solids*. 1984: Elsevier Science Ltd.
9. T. Kundu, ed. *Ultrasonic nondestructive evaluation: engineering and biological material characterization*. 2004, CRC Press.
10. D. Schneider, B. Schultrich, H.J. Scheibe, H. Ziegele, M. Griepentrog, "A laser-acoustic method for testing and classifying hard surface layers", *Thin Solid Films*, vol.332, no.1-2, pp.157-163, November 1998
11. C. Glorieux, W. Gao, S.E. Kruger, K. Van de Rostyne, W. Lauriks, J. Thoen, "Surface acoustic wave depth profiling of elastically inhomogeneous materials", *Journal of Applied Physics*, vol.88, no.7, pp.4394-4400, October 2000
12. H.C. Wang, S. Fleming, Y.C. Lee, "A remote, non-destructive laser ultrasonic material evaluation system with simplified optical fibre interferometer detection", *Journal of Nondestructive Evaluation*, vol.28, no.2, pp.75-83, June 2009
13. H.C. Wang, S. Fleming, Y.C. Lee, S. Law, M. Swain, J. Xue, "Noncontact, nondestructive elasticity evaluation of sound and demineralised human dental enamel using laser ultrasonic surface wave dispersion technique", *Journal of Biomedical Optics*, vol.14, no.5, pp.054046, October 2009
14. H.C. Wang, S. Fleming, Y.C. Lee, S. Law, M. Swain, J. Xue, "Laser ultrasonic surface wave dispersion technique for non-destructive evaluation of human dental enamel", *Optics Express*, vol.17, no.18, pp.15592-15607, August 2009

15. S.J. Davies, C. Edwards, G.S. Taylor, S.B. Palmer, "Laser-generated ultrasound: its properties, mechanisms and multifarious applications", *Journal of Physics D: Applied Physics*, vol.26, no.3, pp.329-348, March 1993
 16. J.D. Achenbach, "Laser excitation of surface wave motion", *Journal of the Mechanics and Physics of Solids*, vol.51, no.11, pp.1885-1902, November 2003
 17. J.L. Rose, *Ultrasonic Waves in Solid Media*. 1999: Cambridge University Press.
 18. J. Kushibiki, K.L. Ha, H. Kato, N. Chubachi, F. Dunn, "Application of Acoustic Microscopy to Dental Material Characterization", *IEEE 1987 Ultrasonics Symposium*, pp.837-842, 1987
 19. S.D. Peck, J.M. Rowe, G.A. Briggs, "Studies on sound and carious enamel with the quantitative acoustic microscope", *Journal of Dental Research*, vol.68, pp.107-112, 1989
 20. J. Arends, J. Christoffersen, "The Nature of Early Caries Lesions in Enamel", *Journal of Dental Research*, vol.65, no.1, pp.2-11, 1986
 21. H.C. Wang, S. Fleming, S. Law, T. Huang. Selection of an appropriate laser wavelength for launching surface acoustic waves on tooth enamel. in *Proceedings of IEEE Australian Conference on Optical Fibre Technology/Australian Optical Society (ACOFT/AOS)*. 2006. Melbourne, Australia.
 22. J.M. ten Cate, P.P. Duijsters, "Influence of fluoride in solution on tooth demineralization. I. Chemical data", *Caries Research*, vol.17, no.3, pp.193-199, 1983
 23. R.G. Maev, L.A. Denisova, E.Y. Maeva, A.A. Denissov, "New Data on Histology and Physico-Mechanical Properties of Human Tooth Tissue obtained with Acoustic Microscopy", *Ultrasound in Medicine and Biology*, vol.28, no.1, pp.131-136, March 2002
 24. D.W. Blodgett, "Applications of laser-based ultrasonics to the characterization of the internal structure of teeth", *Journal of the Acoustical Society of America*, vol.114, no.1, pp.542-549, July 2003
 25. Y. Iijima, O. Takagi, J. Ruben, J. Arends, "In vitro remineralization of in vivo and in vitro formed enamel lesions", *Caries Research*, vol.33, no.3, pp.206-213, 1999
-

1. Introduction

Dental caries is a common disease that results from the excessive mineral dissolution of dental enamel caused by plaque bacteria induced acid [1]. If the development of such demineralisation process can be identified and evaluated at an early stage, reparative approaches, such as enhanced remineralisation using fluoride, can be applied to halt the decay process or even repair the affected tooth structure. However, current clinical diagnostic tools/techniques, such as tactile and X-ray assessments [2], are relatively ineffective for quantifying the level of enamel mineralisation that is important for determining the severity of the demineralisation sites as well as assessing the efficacy of the proposed remineralisation treatments. As a result, application of remineralisation methods is limited and the clinical treatment for dental caries is still dominated by repairing the already damaged tooth structure using invasive surgical interventions.

The level of mineralisation of dental enamel is closely linked to its stiffness and/or elastic response [3-5]. Currently available techniques for quantifying the elastic modulus of teeth, e.g. nano-indentation, involve destructive contact probing which makes repetitive measurements unreliable and it can only be performed on extracted teeth (*in-vitro* measurements) [4, 6]. In this regard, a non-contact and non-destructive technique with the potential for localised *in-vivo* evaluation of the elastic modulus of human dental enamel is desirable.

A Surface Acoustic Wave (SAW) is a type of elastic ultrasound which propagates across a material surface with most of the wave energy, and hence the wave motion, concentrated within a penetration depth similar to its wavelength [7]. The propagation velocity of SAW is particularly sensitive to the elastic constants of all the material layers it probes [8]. Determining the SAW velocity of different frequency components (different penetration depths) yields a dispersion spectrum whose slope and curvature reveal information about the elastic and geometric parameters of the specimen [9-11].

In previous studies we have demonstrated a non-contact, non-destructive elastic evaluation technique utilising the dispersion of laser generated and detected SAW [12] and validated its effectiveness for evaluating the state of elastic response of both sound and demineralised human dental enamel [13-14].

In this paper we demonstrate the significance and capability of this technique with the first report of progressive elasticity evaluation of artificially demineralised human enamel, during a two week remineralisation process. The measurement technique is briefly discussed first, presenting only the key validation results here for background. The elastic properties of human dental enamel are then considered and the measurement results of demineralised and progressively remineralised human enamel are presented and discussed. This preliminary study is the first time, to the best of our knowledge, that such a laser ultrasonic system has been successfully applied, using the evaluation of the elastic response of human dental enamel, to the assessment of the effectiveness of remineralisation treatment; demonstrating its potential to replace or complement existing dental clinical diagnosis methods.

2. Laser ultrasonic technique

2.1 System configuration

Detailed discussion and extensive validation testing results of this laser ultrasonic SAW dispersion technique can be found in a previous publication [12]. Key details only are presented here. The schematic of the measurement system is illustrated in Fig. 1.

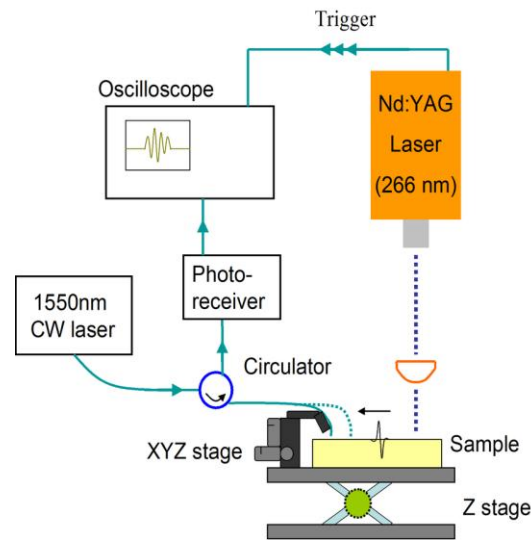


Fig. 1. Arrangement of the laser ultrasonic system for the SAW dispersion measurement.

A solid state Nd:YAG laser operating at 266 nm was used to excite surface waves on the surface of samples. The source laser pulses of ~ 5 ns duration were focused into a thin line by a cylindrical lens onto the sample surface, as shown on the right of Fig. 1. The absorbed electromagnetic radiation from the laser pulse produces localised heating and results in rapid thermo-elastic expansion around the illuminated region, hence generating ultrasound [15-16]. In this measurement setup, test samples were placed on a manual Z-stage and the separation between the lens and the sample was finely tuned such that the line-source width was sufficiently narrow in both the temporal (~ 5 ns) and spatial (~ 80 μm line width) domains so the generated SAW has a broad frequency spectrum and was thus able to probe multiple layers in the material simultaneously. In the current study, the usable frequency bandwidth of the generated SAW (i.e. those frequency components with sufficient signal-to-noise ratio for reliable measurement) typically spanned from 1 \sim 25 MHz [13], equivalent to a probing depth of 3 \sim 0.1 mm for wave speed of ~ 3000 m/s. The bandwidth of the generated SAW could be further increased by reducing the line-source width but this unavoidably raises the irradiating power density, potentially to a level that may damage the specimen surface. During

measurements the laser pulse energy and the sample surface were constantly monitored to ensure no physical damage occurred.

The broadband SAW impulse propagates perpendicular to the line-source and was detected by an Optical Fibre Interferometer (OFI), as shown on the left of the sample in Fig. 1. The OFI consisted of three components joined by fibre connectors: a 1550 nm continuous-wave laser source, a 3-port optical fibre circulator and a photo-receiver. The detected signal was captured by a digital oscilloscope triggered from the Nd:YAG laser. The OFI operates in a similar fashion to a reference beam interferometer [12]. The coherent laser light from the source was coupled into the circulator. As the light arrives at the end of the cleaved middle port (the sensing tip), it is split into the reference and measurement beams by partial internal reflection (from the fibre tip) and subsequently the measurement beam is returned by external reflection (from the tooth surface). The two beams co-propagate back into the sensing fibre and toward the photo-receiver at the third port. This common path environment means that the path difference of the two beams, and hence their relative phase, depends only on the separation between the fibre tip and the sample surface (the measurement beam path-length). In a typical ultrasonic measurement the elastic wave induced surface vibration modulates the measurement beam path-length with an amplitude less than a quarter of the OFI source wavelength, which means that the phase modulation is less than π and the interference intensity becomes a good measure of the absolute acoustic waveform.

The sensing port of the circulator was placed on a micron-precision three axis (XYZ) positioning-stage (0.1 μm precision) such that the probe-to-sample separation can be adjusted to optimise the returning signal strength and the spatial resolution, as well as making measurements at different locations. All measurements were made with a probe-to-sample separation of 5 mm or smaller such that the measurement beam was formed predominately by the reflection off a small area directly beneath the fibre centre. This means that the actual measurement beam size was similar to the fibre core, about 8 μm , and was small compared to the generated ultrasonic wavelength (0.1 ~ 3 mm), hence ensuring a negligible averaging effect for truly point to point measurements. This positioning-stage permits measurements between 1 mm and 12 mm from the line-source. The propagating SAWs were recorded at various locations along the epicentral axis of the line-source and digitally filtered to reduce low and high frequency noise. Typically we use the largest possible measurement spot separation for analysis, for example in the enamel measurement we used 3.5 mm separation (1 mm to 4.5 mm away from line-source).

2.2 Surface wave dispersion analysis

The wave motion and hence the propagation velocity of the SAW, c_R , is governed by the elastic properties of the material layers within the frequency dependent penetration depth. The SAW penetration depth, z , can be estimated from the relation [8, 17]:

$$z \approx c_R / f, \quad (1)$$

where f is the SAW frequency. As a broadband SAW propagates along a material surface, the higher frequency components have shallow penetration depth and are more influenced by the elastic parameters of the surface layer. On the other hand, the lower frequency components penetrate deeper and are influenced more by the bulk elastic parameters. Typically c_R is proportional to the elastic modulus but inversely proportional to the density [8]. In an isotropic homogeneous medium c_R is independent of the penetration depth (having a constant value for all frequency components) as well as propagation direction. In a complex inhomogeneous medium c_R becomes a function of signal frequency and the SAW is dispersed [17]. The characteristics of the dispersion curves depend on the nature of the specimen.

In this study, the experimental frequency dependent c_R and hence the dispersion curve was determined from two of the measured SAW signals, having furthest separation at locations x_1 and x_2 , using the following equation [12]:

$$c_R(f) = 2\pi f \frac{x_2 - x_1}{\varphi(f)}, \quad (2)$$

where f is the SAW frequency and $\varphi(f)$ is the phase difference between the two signals derived from their Fourier spectra. Computer code was written to correct the 2π ambiguity of the phase value and derive an accumulating phase sequence.

2.3 Experimental validation of the technique

In this section we briefly present the validation result of a dispersive two-layer medium that is geometrically most relevant to the human tooth structure within the scope of our intended investigation (a lesion layer on top of sound enamel). More extensive validation results of this technique can again be found in reference [12].

A sample composed of a $\sim 40 \mu\text{m}$ thick nickel film ($c_R \sim 2700 \text{ ms}^{-1}$) sputtered onto a thick fused quartz glass substrate ($c_R \sim 3400 \text{ ms}^{-1}$) was used. The measurement and analysis procedures were as discussed above. The experimental dispersion curve is plotted in Fig. 2. Within the reliable bandwidth (1 ~ 20 MHz), the shape of the dispersion curve matches well with the qualitative expectation of the interaction between the ultrasound and the physical structure: the low frequency components travel with a velocity close to that of the glass and the velocity gradually decreases as the wave becomes more influenced by the nickel film at higher frequencies.

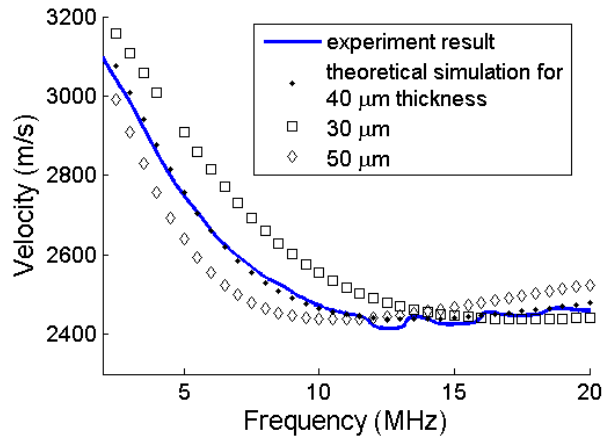


Figure 2: Experimental and theoretical dispersion curves for nickel film on glass substrate.

The partial wave technique [17] was used to calculate the theoretical SAW dispersion spectra using known parameters of the two substances with different film thicknesses (30 μm , 40 μm and 50 μm), also displayed in Fig. 2. The 40 μm simulation is clearly the best fit to the experimental curve and confirmed its accuracy.

The above result demonstrates that the curvature and the trend of the experimental dispersion curve are sufficiently accurate in terms of revealing the state of elastic behaviour of the medium in which the SAW propagates and, most importantly, the elastic response as a function of depth. The main source of uncertainty in this technique will most likely be the error in measuring the signal separations from the OFI translation stage manual micrometer adjustment.

3. Evaluation of human dental enamel

3.1 Elastic and opto-thermal properties of human enamel

Dental enamel consists of unevenly distributed mineral composition and highly oriented microstructure, which results in anisotropic and inhomogeneous mechanical and elastic properties [4]. Kushibiki et al. [18] used line-focused-beam scanning acoustic microscopy and measured the SAW velocity as a function of propagation direction on the labial surface of extracted human incisors and reported that the velocity value varied between 3105 ms^{-1} to 3155 ms^{-1} with the maximum obtained in the direction parallel to the tooth axis (i.e. the direction from crown to root). Peck and colleagues [19] repeated the investigation on the surface of human permanent molars and reported that the SAW velocity varied between 3075 ms^{-1} to 3142 ms^{-1} with the maximum velocity also in the direction parallel to the tooth axis.

An early caries lesion on the surface of enamel is observed clinically as a white opaque spot, and hence referred to as a white spot lesion (WSL) [20]. The surface layer of the WSL is porous but remains relatively intact and mineral rich, however the subsurface area under the WSL (the body of the lesion) is low in mineral (10 ~ 70% of the value for sound enamel). The WSL enamel thus has lower elastic modulus than that of sound enamel and consequently lower SAW velocity. A WSL layer developed on top of sound enamel essentially simulates the two-layer system example discussed in Sec. 2.3 and dispersion is expected when a broadband SAW propagates through such medium.

Prior to actual measurement, a laser absorption spectrum study was conducted and found that the UV light was well absorbed by human enamel [21], hence 266 nm emission from the Nd:YAG laser was chosen for SAW generation. The laser damage threshold for enamel at this wavelength was experimentally determined by irradiating a tooth sample with a line-source of laser pulse energy $\sim 1 \text{ mJ}$ (measured with an optical power-meter after the cylindrical lens) and gradually focusing the line-source until thermal damage (predominately ablation) was observed to occur on the enamel surface. The corresponding line-source dimension was measured with a microscope to be $\sim 1.4 \text{ mm}$ by $\sim 0.02 \text{ mm}$ giving a power density of $\sim 7.5 \times 10^8 \text{ Wcm}^{-2}$ for the damage threshold. For the measurements of human dental enamel, presented below, we operated at a power density value that is well below this measured threshold thus ensuring non-destructive evaluation of the tooth samples.

3.2 Sample preparation

A recently extracted sound human incisor was selected for this initial study because this type of tooth has a large flat area of enamel on its front surface. In addition, the enamel thickness is relatively constant ($\sim 1 \text{ mm}$) over a wide region near the centre of the incisor front surface. This is desirable because the measured SAW dispersion will not depend significantly on the uneven thickness of the enamel layer but rather on the elasticity variation. The sample was stored in deionized water to maintain its *in vivo* condition and only removed during measurement.

An artificial WSL, which is similar to a natural WSL and widely used for dental research [20], was created on the sample. About $\sim 70\%$ of the front surface of the incisor was first abraded and polished approximately to a depth of $\sim 100 \mu\text{m}$ below the natural surface with 400 grit abrasive papers. The procedure was carefully performed such that the sample was still considered to be close to an *in-vivo* condition. A window of about 3 mm by 3 mm was left exposed on the polished region while the rest of the tooth was coated and protected with nail varnish. The sample was then placed in prepared demineralisation solution containing 2.2 mM $\text{Ca}(\text{NO}_3)_2$, 2.2 mM KH_2PO_4 , and 50 mM acetic acid (pH = 4.5) [22] for five days. After the demineralisation treatment, the nail varnish was removed with acetone and the sample was rinsed with distilled water.

3.3 Measurement of sound and demineralised enamel

The first measurement was performed on the healthy region of the sample, as depicted in Fig. 3(a). Due to the limit of usable sound enamel area, the line-source (illustrated as the solid line) was irradiated near the edge of the enamel surface and the SAW propagated in the direction horizontal to the tooth axis. The recording of the surface waves was made at several positions along the propagation path (illustrated as the dots). The measurement was repeated ten times and each time the sample position was shifted randomly by a small amount ($\sim \pm 0.2$ mm) in the direction perpendicular to the wave propagation path, such that the final evaluation result will be the averaged contribution from an area of rectangular shape with ~ 0.4 mm width.

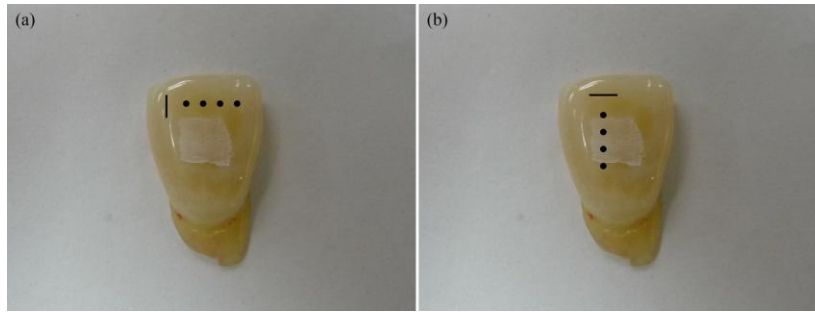


Figure 3: Illustrations showing the positions of the SAW generation and detection on (a) the healthy region and (b) the WSL region of the tooth sample.

For the measurements on the WSL region, as illustrated in Fig. 3(b), we irradiated the line-source near the top edge of the tooth and allowed propagation across the lesion in the direction parallel to the tooth axis. Surface waves were recorded at various locations especially near the junctions of the sound enamel and the WSL (illustrated by the dots). Once again ten measurements, each with small random position variations, were repeated. Dispersion spectra of sound enamel and WSL measurements were calculated and the (ten measurement) averaged values were used as the final results and are presented in Fig. 4 with standard deviation error-bars. It is important to note here that we only investigated frequency components between 7 ~ 25 MHz, which have estimated penetration depths of 0.5 ~ 0.1 mm (using Eq. 1 and $c_R = 3100 \text{ ms}^{-1}$). Frequency components of 1 ~ 7 MHz have deeper penetration depth and were significantly influenced by the underlying dentin, which has lower SAW velocity value than the enamel [23-24]. The influence of dentin on SAW propagation has been reported previously [13] and is not important for this study.

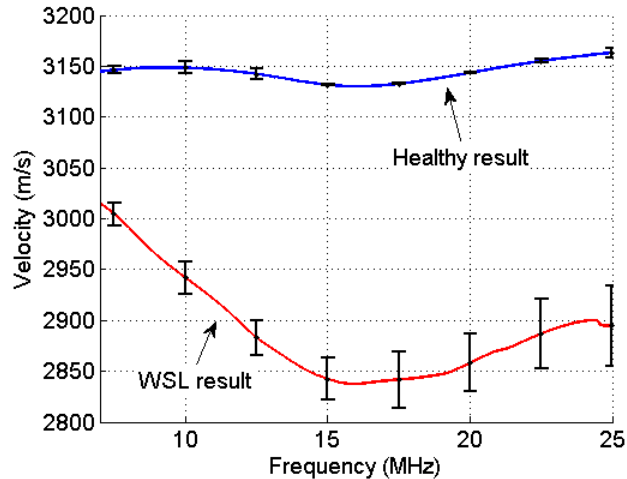


Figure 4: Dispersion curves of the final averaged results from the healthy region (blue) and the WSL region (red) of the sample enamel.

In the sound enamel the SAW propagates as in a relatively homogeneous bulk system and the velocity remains fairly constant at $\sim 3150 \text{ ms}^{-1}$. This value compares well with previously reported values [18-19]. In the WSL region, the contribution from the lower elastic lesion layer (of unknown thickness at this stage) results in a slower initial SAW velocity value which continues to drop as the influence of the lesion layer became more dominant for higher frequency components. This dispersion profile is similar to the example shown in Fig. 2 and fits well with expectation. These results demonstrated that the state of mineralisation of human dental enamel can be evaluated using the laser ultrasonic SAW dispersion method. The differences between the two dispersion spectra are significant (about 10 % drop in velocity value) and clearly discriminate the two types of enamel condition. More detailed and comparison results of sound and demineralised enamel are reported in reference [13].

The enamel anisotropy, as discussed in Sec. 3.1, is insignificant for this study because the maximum SAW velocity on human enamel is in the direction parallel to the tooth axis [18-19]. This suggests that if the sound region measurements of the current study were also performed in the direction parallel to tooth axis, a slightly higher velocity value would be obtained increasing the difference between the WSL and the sound enamel dispersion curves.

3.4 Measurement of enamel remineralisation

Having demonstrated the ability of the laser ultrasonic technique in evaluating and differentiating sound and demineralised enamels, we extended the study to measure, for the first time, the progressive elasticity variation of artificially demineralised human enamel during remineralisation treatment.

Remineralisation solution (pH = 7.0) was prepared containing 20 mM HEPES buffering agent, 1.50 mM calcium chloride dihydrate, 0.90 mM potassium dihydrogen orthophosphate and 1 ppm fluoride as NaF [25]. The same incisor sample used in Sec. 3.3, which had been demineralised for 5 days, was again used in this study. It was soaked entirely in the remineralisation solution for two weeks, the solution being renewed after the first week. Four sets of ten measurements were taken during the two week period after 4, 7, 10 and 14 days of treatment. Prior to each set of measurements the sample was taken out of the remineralisation solution, washed with distilled water and left to dry in air. The measurement procedure, including the measurement regions, and the dispersion analysis were identical to that in Sec. 3.3. Again we restricted our analysis to signals within the frequency band of 7 ~ 25 MHz.

The final averaged dispersion curves (ten measurements for each set) of the sound enamel and the WSL measurements after 4, 7, 10 and 14 days of remineralisation are shown in Fig. 5

and 6, respectively (with different vertical scales). For comparison, the original non-remineralised results are also included in the corresponding figures. All of the results have less than 3 % standard deviation and the error-bars are not shown for the clarity of the figures.

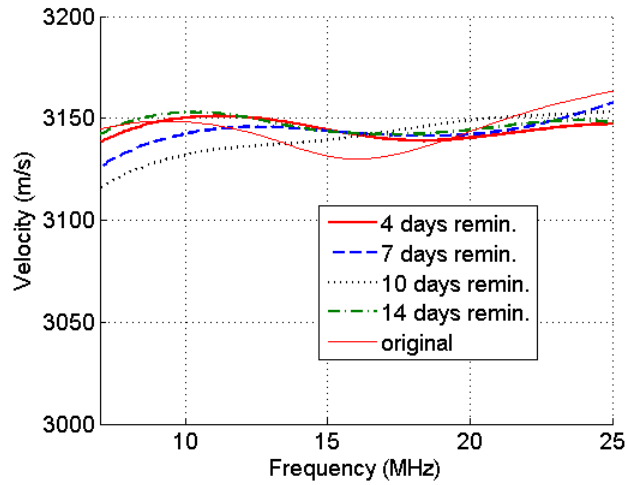


Figure 5: Comparison diagram of the sound enamel results during the two weeks remineralisation treatment.

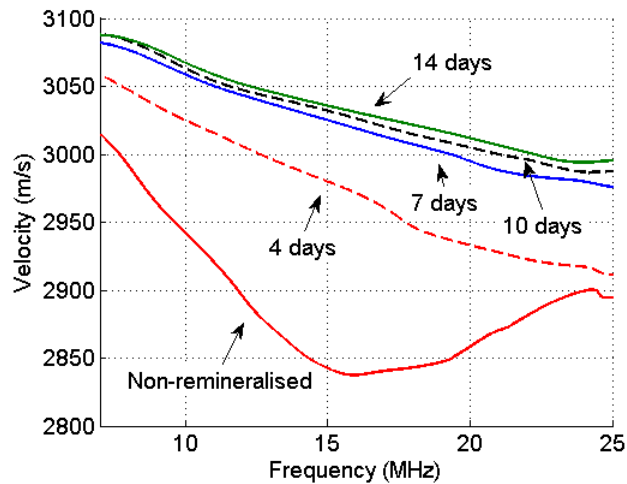


Figure 6: Comparison diagram of the WSL results from the two weeks remineralisation treatment.

For the sound enamel the SAW velocities are almost unchanged at $\sim 3150 \text{ ms}^{-1}$ (less than 1% variation) during the two weeks of remineralisation treatment, which indicates that the treatment causes no change in the sound enamel. On the other hand, some interesting and significant changes can be observed from the WSL results. First and foremost, there is a trend towards increasing velocity values in the dispersion curves as the number of days of remineralisation increases. This rise is most significant in the first week of the remineralisation treatment with the velocity increasing by $\sim 60 \text{ ms}^{-1}$ near 7 MHz and almost 160 ms^{-1} at $\sim 16 \text{ MHz}$. This observation clearly suggests that the elastic modulus of the lesion layer has increased in value during the first 7 days of remineralisation. In the second week of

the treatment, the increase in SAW velocity is minimal, which could be explained by a saturation of the remineralisation process.

To verify the accuracy of the ultrasonic results as well as the state of the lesion layer, a cross-sectional nano-indentation investigation was performed on the incisor sample after completion of the laser ultrasonic measurements. The tooth was sectioned through the measured WSL region and mounted in epoxy. The enamel thickness was measured with a digital micrometer to be ~ 1.2 mm near the crown and relatively constant at ~ 1 mm throughout the centre region where the measurements were taken. Five sets of nano-indentation measurements were performed, evenly along the length of the WSL. The indentation of each set starts from the surface and proceeds to a depth of $280 \mu\text{m}$ below the enamel surface at $20 \mu\text{m}$ spacing. A microscope photograph was taken during the nano-indentation (Fig. 7) where the enamel is shown on the left hand side and the epoxy is on the right hand side. The junction region with abrasion marks is the artificial lesion and a small amount of void appears black.

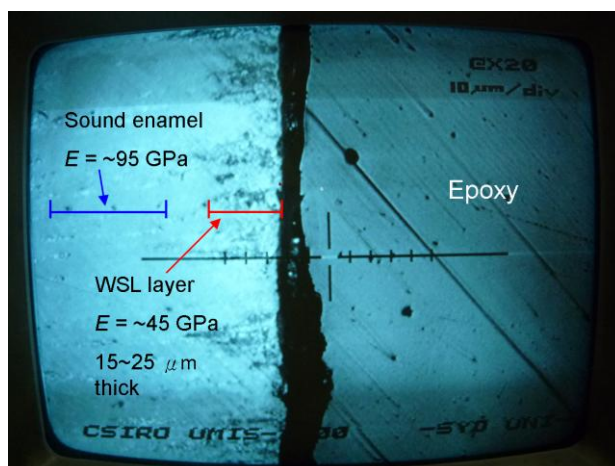


Figure 7: Microscope photo taken during the nano-indentation on the centre of the artificial WSL.

The elastic modulus of the healthy bulk enamel was measured and averaged over 30 indentations to be 92.5 ± 1 GPa. As seen in Fig. 7, the lesion layer has a varying thickness of $15 \sim 25 \mu\text{m}$ and the mean elastic modulus of 6 indentations in the lesion region is 42.7 ± 6 GPa. These parameters pertain to the state of the tooth sample after 14 days remineralisation and we used them to plot simulated dispersion curves to further verify the experimental result. Two simulations were plotted using the same algorithm as in Sec. 2.3. The first simulation was for a single layer medium modeling only the healthy enamel. The second simulation was for a two-layer medium consisting of a less elastic surface ($20 \mu\text{m}$ thick) on top of the sound enamel substrate. The first simulation was fitted to the experimental curve of the sound enamel using a computer algorithm and a best fit elastic modulus value of 92.8 GPa was obtained. This value was then used as the substrate parameter when fitting the second simulation to the experimental WSL curve and the best fit elastic modulus value for a $20 \mu\text{m}$ thick lesion layer was determined to be 43.2 GPa. Fig. 8 shows the simulated and experimental dispersion curves for the sound enamel and WSL. It is obvious that the fitted theoretical curves display similar profiles to the experimental results for both sound enamel and WSL and the parameters found to give the best fit compare well to those measured from the nano-indentation measurements within standard error.

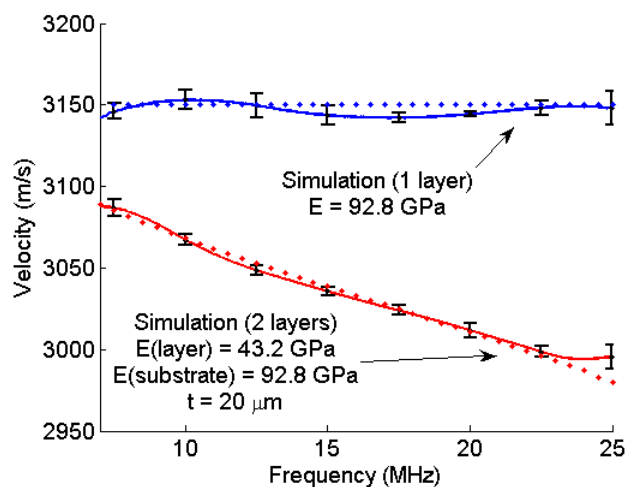


Figure 8: Comparison between theoretical simulations and the 14 days remineralised enamel results (with standard deviation error-bars).

From these results it is clear that we have successfully evaluated the change in the SAW dispersion curves, which directly correlate to the elastic properties, of a human tooth under remineralisation treatment.

4. Conclusion

In this paper we presented the latest advances in the application of a recently demonstrated laser ultrasonic technique that utilises laser generated and detected SAW to provide non-destructive elasticity evaluation of surface materials. This technique has been demonstrated to evaluate healthy and demineralised human dental enamel and quantitatively distinguish their elastic response. In this work we demonstrated that this technique is sufficiently sensitive to be able to perform progressive monitoring of a remineralisation process. It was apparent that the SAW velocity increased only in the demineralised region. Theoretical simulations were fitted to the final result from the 14 days remineralised enamel. The elastic modulus values which produced the best fit compared well to the results of nano-indentation tests on the tooth. This is the first time, to the best of our knowledge, that such a laser ultrasonic system has been successfully applied to assess the human dental enamel elastic variation during a remineralisation treatment.

Although *in-vivo* tests have not yet been performed, the laser ultrasonic technique is a good candidate as a new examination tool for dental research purposes. Contrasted with the conventional destructive nano-indentation method and the limited discrimination provided by X-ray procedures, laser ultrasound provides repeatable non-destructive evaluation which can be used to study dental lesions of different severity and depth. We have also shown that it is potentially a valuable tool for verifying the efficacy of different remineralisation methods and even investigating the nature and progress of the remineralisation process.

Acknowledgement

This work was funded by the Australian Government and Bio-Dental Technology Pty. Ltd. under an ARC Linkage Grant, No. LP0561184.